Electronic Supplementary Material (ESI) for Physical Chemistry Chemical Physics.

SUPPORTING INFORMATION

A Comparison of the Solvation Structure and Dynamics of the Lithium Ion in Linear Organic Carbonates with Different Alkyl Chain Lengths

Kristen D. Fulfer and Daniel G. Kuroda

Modified Sample Cell Used for 2DIR Experiments

A diagram of the modified sample cell, utilizing a CaF_2 convex lens is shown below.

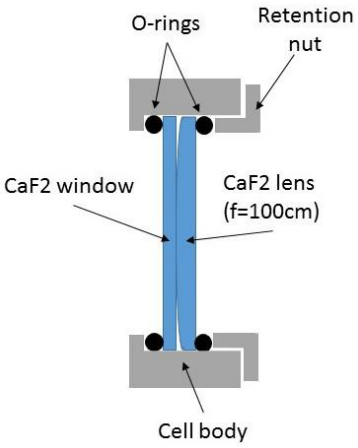

Figure S1. Labeled diagram of the modified sample cell used for 2DIR.

DFT Calculations Justifying the Use of the Vibrational Exciton Model vs the Local Mode Model

In order to justify the use of a vibrational exciton model as opposed to using local modes to describe the carbonyl stretches of the carbonates solvating the Li^+, gas phase density functional theory calculations were performed. The following four systems (1) a free DMC molecule with the carbonyl group isotopically labeled ($^{13}C{=}^{18}O$), (2) Li^+ tetrahedrally solvated by four DMC molecules with one DMC molecule isotopically labeled ($^{13}C{=}^{18}O$), (3) Li^+ tetrahedrally solvated by four DMC molecules with two DMC molecules isotopically labeled ($^{13}C{=}^{18}O$), and (4) Li^+ tetrahedrally solvated by four DMC molecules with all four DMC molecules isotopically labeled ($^{13}C{=}^{18}O$). Calculation (1) gives the free $^{13}C{=}^{18}O$ stretch of DMC, (2) gives the coordinated DMC $^{13}C{=}^{18}O$ stretch local mode, (3) gives the vibrational exciton modes generated by the two labeled DMC molecules (exciton2), and (4) gives the vibrational exciton modes generated by the four labeled DMC molecules (exciton4). The resulting frequencies and intensities from calculations (1-4) are shown below.

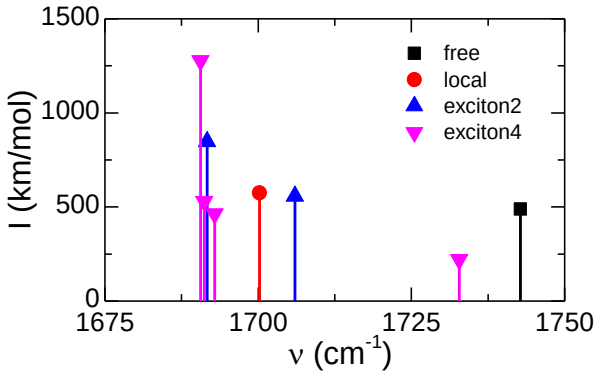

Figure S2. Calculated frequencies and intensities for the free $^{13}C{=}^{18}O$ stretch (calculation 1), the local coordinated $^{13}C{=}^{18}O$ stretch (calculation 2), the vibrational exciton modes from two $^{13}C{=}^{18}O$ (calculation 3) and the vibrational exciton modes from four $^{13}C{=}^{18}O$ (calculation 4).

FTIR spectra of linear carbonates in organic solvents

Since the Fermi resonances are known to affect the carbonyl stretch region of the infrared spectrum for many of the cyclic carbonates, the linear carbonates were checked for evidence of Fermi resonances in this region as well. Each of the linear carbonates were diluted in organic solvents such as tetrahydrofuran (THF), dimethylsulfoxide (DMSO), and hexanes. The FTIR data present no evidence of Fermi resonances in the carbonyl stretch region for DMC, EMC, or DEC.

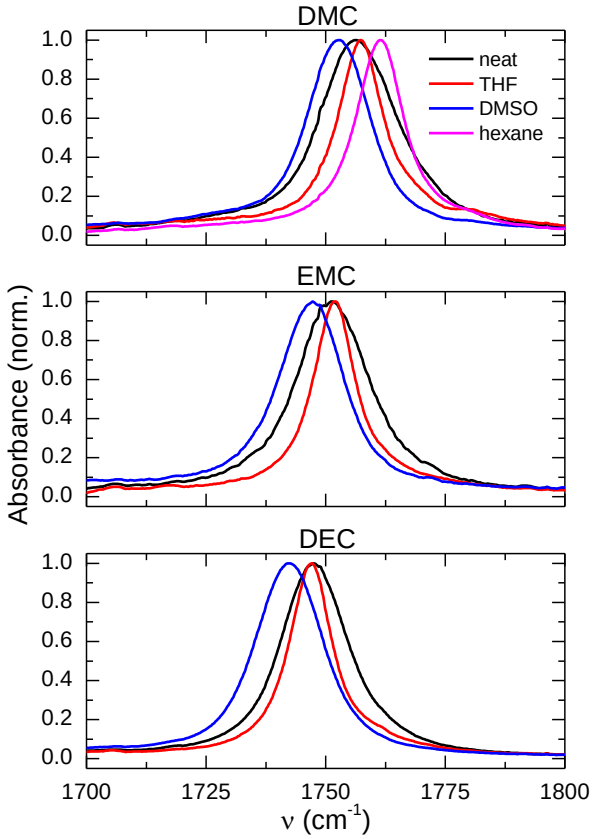

Figure S3. FTIR spectra of the carbonyl stretch region for DMC, EMC, and DEC diluted in various organic solvents.

Effects of the Presence of Water on the Carbonyl Stretch

In order to investigate the effects of the presence of a small amount of water on the dynamics of the Li^+ solvation shell, one drop of water was added to approximately 0.5 mL of a solution of LiPF6 in DMC with $X(LiPF_6)=0.09$. FTIR of the wet and dry solutions are shown below. It is apparent that small amount of water present in the solution do not have a large effect on the carbonyl stretch region of the IR spectrum. The main difference seen in the FTIR is a small shift (<5 cm^{-1}) to higher frequency of the coordinated band.

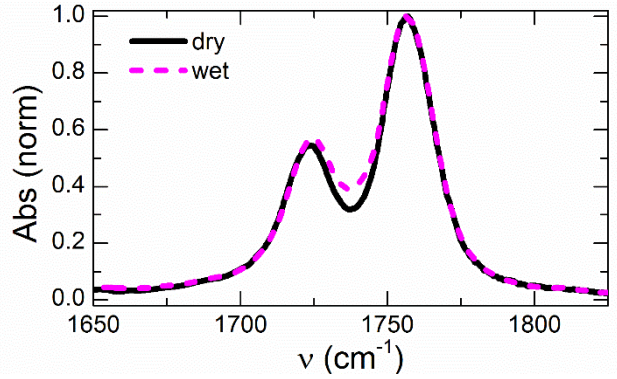

Figure S4. FTIR spectra of the carbonyl stretch region for $LiPF_6$ in DMC with $X(LiPF_6)=0.09$ both without (black, solid line) and with (pink, dashed line) a small amount of additional water.

The effects of the presence of water on the dynamics of the Li^+ solvation shell were also studied via 2DIR. The results of modelling the inverse CLS of the 2DIR data as a function of waiting time for both the wet and dry solutions are summarized in the table below. While the vertical offsets, which represent either slow dynamics relative to the 5 ps of waiting time measured or the presence of multiple transitions, are decreased slightly in the presence of water, the characteristic times, τ_1, do not seem to be affected.

Table S1. Resulting parameters from modelling the inverse CLS of the 2DIR for the wet and dry LiPF6 in DMC solutions as a single exponential decay.

Solution	Free Carbonyl Stretch		Coordinated Carbonyl Stretch	
	τ_1 (ps)	y0	τ_1 (ps)	y0
Wet	1.7±0.1	0.08±0.01	1.6±0.1	0.14±0.01
Dry	1.9±0.2	0.13±0.02	1.4±0.1	0.25±0.01

Spectral Signatures of the Contact Ion Pair in the 2DIR Data

In order to distinguish the spectral signatures in the carbonyl stretch region of contact ion pairs, 2DIR was employed, since 2DIR has increased spectral resolution. Solutions of $LiPF_6$ in DMC with $X(LiPF_6)=0.09$, which was the concentration used throughout the paper, and $X(LiPF_6)=0.30$ were compared. In the solution with a Li^+ mole fraction of 0.30, there are only 2.3 carbonates per Li^+, meaning there are not enough carbonates to tetrahedrally solvate each Li^+. This shortage of available carbonate molecules should force the formation of contact ion pairs. The 2DIR at waiting time 2 ps is shown below for both $LiPF_6$ concentrations. It is apparent in the $X(LiPF_6)=0.30$ solution that the coordinated carbonyl stretch is shifted to higher frequency by approximately 3 cm-1. Also, there are two sets of cross peaks with the coordinated band in the higher frequency data, indicating a splitting of the free carbonyl stretch band. This is better illustrated by comparing the horizontal traces through the coordinated diagonal band for each spectrum, also shown below. In the high concentration data, as evidenced by the cross peaks, the free carbonyl stretch is split to ω_τ = 1758 and 1771 cm^{-1} from ω_τ = 1767 cm^{-1} in the lower concentration solution. Since in the high concentration there are not enough carbonates to fully solvate the Li^+, contact ion pairs must form. Thus, this splitting of the high frequency transition in the carbonyl stretch region is attributed to the presence of contact ion pairs. Furthermore, since this peak splitting is not evident in any of the 2DIR data for the solutions used in the paper, it is assumed that the presence of contact ion pairs in the solutions studied is negligible.

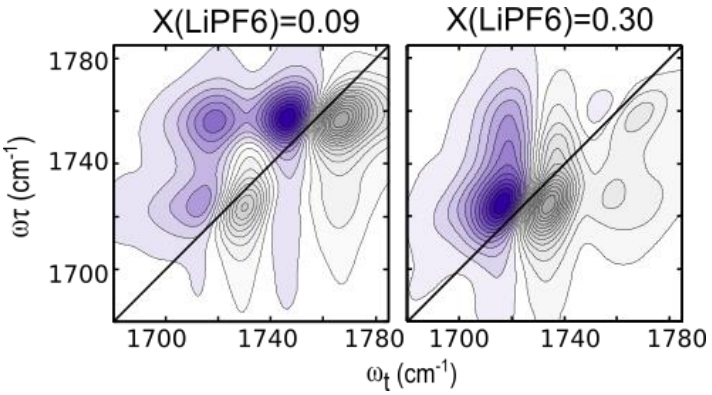

Figure S5. 2DIR spectra at T_w=2 ps for $LiPF_6$ in DMC at $X(LiPF_6)=0.09$ and $X(LiPF_6)=0.30$.

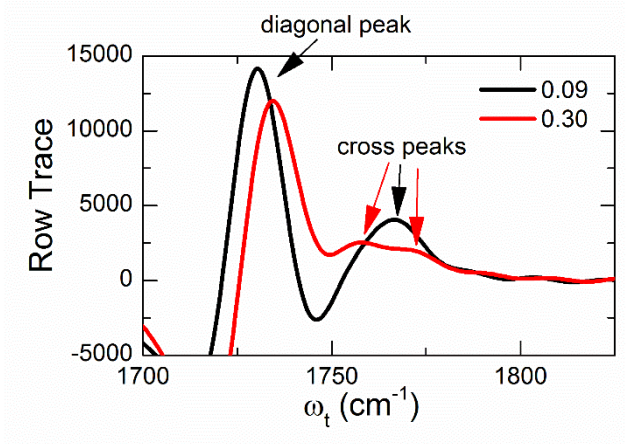

Figure S6. Horizontal traces through the coordinated carbonyl stretch diagonal peak at T_w=2 ps for $LiPF_6$ in DMC at $X(LiPF_6)=0.09$ and $X(LiPF_6)=0.30$.

Gas phase DFT calculations were also performed to show that the spectral signatures of solvation shells consisting of only three carbonates or of the contact ion pairs (CIP) were also performed. In Figure S7, the DFT calculated C=O stretch frequencies and intensities with 1 Li+ and three DMC molecules in a trigonal planar configuration are shown as Li3DMC, while the Li3DMC_tet structure consists of a Li+ solvated by 2 DMC molecules through the carbonyl groups and 1 DMC molecule through the two ethereal oxygens. For the CIP structures in Figure S8, the CIP(mono) structure consists of Li+ solvated by three DMC molecules and 1 PF6-, where only one of the F atoms is interacting with the Li+. However, the CIP(bi) structure consists of 1 Li+ solvated by two DMC molecules and interacting with 2 F atoms from the PF6- anion. In either case (only 3 DMC in the solvation shell or the formation of CIP), it can be seen that there is no longer a coupled C=O stretch from

the solvation shell which is frequency overlapped with the free carbonate; thus, the cross peaks between the free and coordinated C=O bands would not be present in the 2DIR spectra.

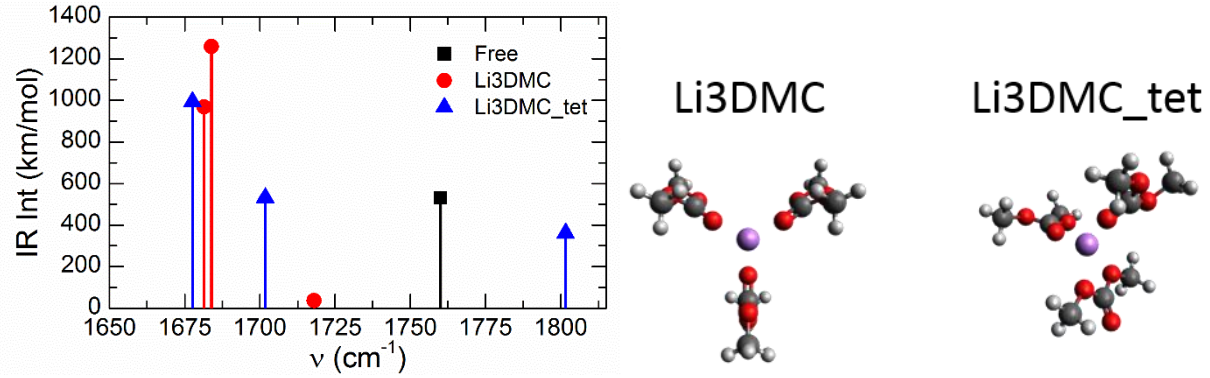

Figure S7. Calculated frequencies and IR intensities of the C=O stretch modes arising from the solvation shells containing 3 DMC. Structures shown to the right.

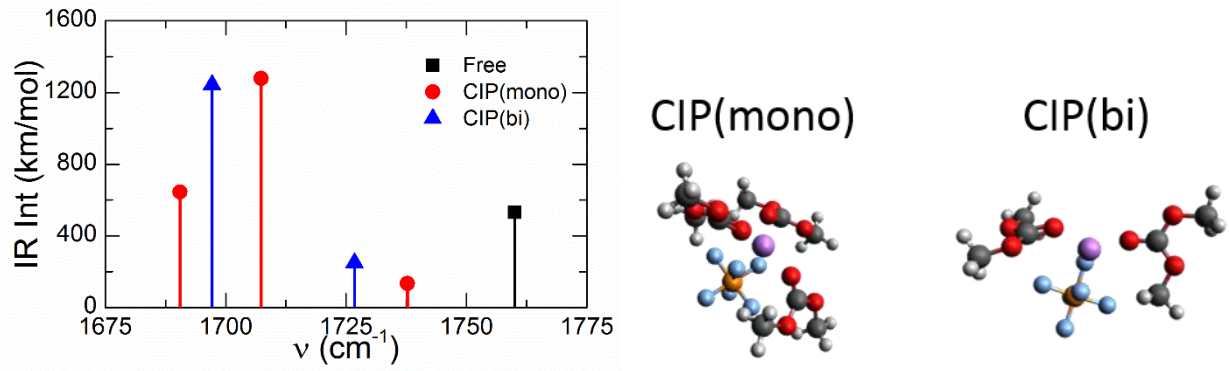

Figure S8. Calculated frequencies and IR intensities of the C=O stretch modes arising from the contact ion pair solvation shells. Structures shown to the right.

Model of the FTIR data

The two bands in the FTIR data for $LiPF_6$ in each of DMC, EMC and DEC were modeled with Voigt profiles. Table S2 shows the fitting parameters used for each band of all three electrolytes.

TABLE S2. Fitting parameters FTIR data for $LiPF_6$ in DMC, EMC, and DEC at $X(LiPF_6) = 0.09$. All frequencies and widths are reported in cm^{-1}. The carbonyl stretch region of each spectrum was modeled with two Voigt profiles, denoted as the free and Li^+-coordinated bands.

Solvent	Free Band				Li+-Coordinated Band			
	Freq.	FWHM	Gaussian Width	Lorentz. Width	Freq.	FWHM	Gaussian Width	Lorentz. Width
DMC	1757.1	23.1±0.1	13.8	11.3	1723.8	22.7±0.4	5.7	20.6
EMC	1752.1	21.0±0.1	10.3	13.7	1719.5	30.0±0.5	19.6	11.7
DEC	1747.3	19.7±0.2	7.4	15.7	1714.0	26.3±0.8	13.4	16.4

2DIR Data at Zero Waiting Time with k_1 and k_2 at 45°

2DIR data were collected for zero waiting time with k_1 and k_2 set to 45° in order to amplify the off-diagonal features due to vibrational coupling in the DMC and DEC electrolytes. The cross peaks at T_w=o are very evident in this data further evidencing the presence of vibrational coupling.

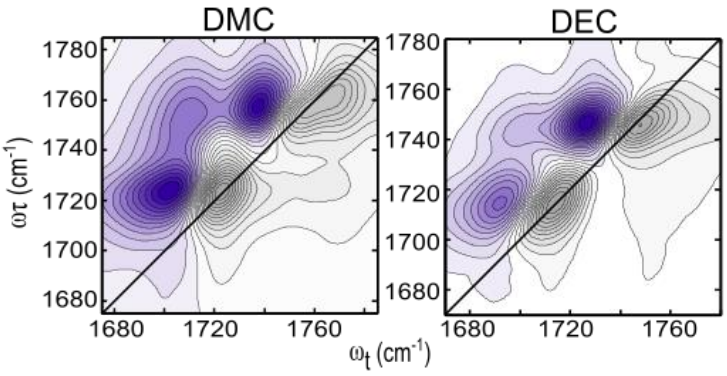

Figure S9. 2DIR data at zero waiting time for the DMC and DEC electrolytes. This data was collected with k_1 and k_2 at 45°.

Calculated IR transition strength of the carbonyl stretch

The carbonyl stretch frequencies and IR strengths were calculated for each of the pure carbonates and as well as the single Li^+-carbonate interaction for each of the three linear carbonates: DMC, EMC, and DEC, using gas-phase DFT. Table S3 shows the results for each of these calculations. The Li^+-carbonate frequencies and IR intensities were calculated for the optimized θ angle (DMC: θ = 148.1°, EMC: θ = 147.6°, and DEC: θ = 145.8°). For each of these calculations only a single carbonate was used for the calculation.

TABLE S3. Calculated frequencies and IR intensities of the carbonyl stretch for each pure carbonate as well as for each single Li^+-carbonate interaction from gas-phase DFT.

Solvent	Free Carbonate		Li^+-Carbonate	
	Freq. (cm^{-1})	IR Intensity (km/mol)	Freq. (cm^{-1})	IR Intensity (km/mol)
DMC	1823.5	529.7	1698.6	714.7
EMC	1818.7	530.0	1690.5	720.9
DEC	1812.6	513.3	1680.8	671.6

The ratio of the free band to the coordinated band of the carbonyl stretch region was also calculated using DFT for the free Li+ solvation shell (tetrahedral), the solvent separated ion pair (SSIP), and the contact ion pair (CIP) for DMC. The free Li+ solvation shell consisted of 1 Li^+ and 4 DMC molecules; the SSIP consisted of 1 Li^+, 1 $PF6^-$, and 4 DMC molecules; and the CIP consisted of 1 Li^+, 1 $PF6^-$, and 3 DMC molecules. These results are shown in Table S4. The ratio of the bands in the carbonyl stretch region of the infrared spectrum should be insensitive to the species present (free, solvent separated ion pair, or contact ion pair) according to DFT calculations.

Table S4. Calculated ratio of IR intensities for the free carbonyl stretch to the coordinated carbonyl stretch for the free solvation shell, the solvent separated ion pair (SSIP), and the contact ion pair (CIP) for $LiPF_6$ in DMC.

	Free	SSIP	CIP
Free/Coordinated Ratio	0.78	0.79	0.75

Amplitude of frequency fluctuations

According to Kubo's lineshape theory, the FFCF of the coordinated carbonyl stretch in each electrolyte can be modeled as

$$FFCF(t) = \Delta_1^2 e^{(-t/\tau_1)} + \Delta_2^2$$

Where Δ_1 is the amplitude of the frequency fluctuations which is directly related to the disorder of the system, Δ_2 is the static inhomogenous term, and τ_1 is the frequency decorrelation characteristic time. By modeling the FTIR using the FFCF above, the amplitudes of fluctuation may be calculated. The Δ_1 values obtained for the asymmetric carbonyl stretch of the Li+-solvation shells formed in each electrolyte are shown in the table below.

TABLE S4. Amplitude of fluctuation (Δ_1) in ps^{-1} for each of the three electrolytes.

Solvent	Δ_1 (ps^{-1})
DMC	2.0
EMC	2.5
DEC	2.2

ATR-FTIR of the P-F stretch modes

ATR-FTIR spectra of the P-F stretch modes were collected for each electrolyte to compare the environment of the PF_6^- anion. The P-F stretch modes from each electrolyte are quite similar, all showing three bands between 810 and 890 cm^{-1}. The band at ~840 cm^{-1} has been assigned to the PF_6^- anions solvated by carbonate molecules (or the free PF_6^- anions), while the side bands at ~825 cm^{-1} and ~865 cm^{-1} are assigned to ion pairs, though the there is some disagreement as to the type of ion pair.[1, 2] However, from the carbonyl region of the 2DIR, the presence of a significant amount of contact ion pairs can be disregarded, thus, it is assumed that majority of the Li+ is found either freely solvated or as are solvent separated ion pairs (see Chart 3 in the manuscript). Qualitatively, the ATR spectra show that $LiPF_6$ has similar ion pair formation in the three linear carbonate solvents investigated, though a full lineshape analysis was not performed on the P-F stretch modes due to the difficulty of separating the solvent bands in the cases of EMC and DEC and due to reliability issues of ATR lineshape analysis.

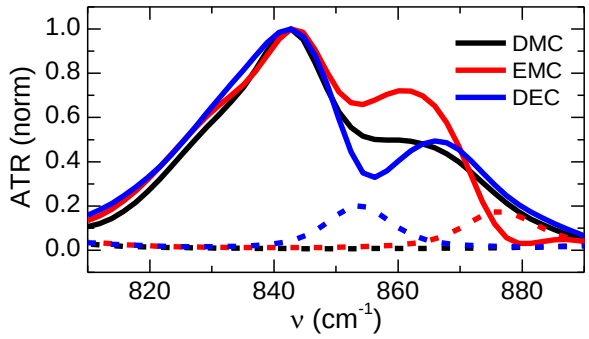

Figure S10. ATR-FTIR spectra for all three electrolytes (normalized and shown as solid lines) with background (neat solvents) subtracted. ATR spectra of the neat solvents are shown as dashed lines (not normalized) for reference.

Vibrational lifetimes of the Li^+-coordinated carbonyl stretch

The sum of the absolute values of the peak areas in the τ_ω trace which intersects the maximum of the diagonal peak was plotted as a function of waiting time, T_w, as shown in Figure S9. These curves were then modelled with an exponential decay of the form: $A * e^{-T_w/T_1} + y0$, where T_1 is the vibrational lifetime of the Li^+-coordinated carbonyl stretch. Table S5 contains the fitting parameters used to model the data shown in Figure S9.

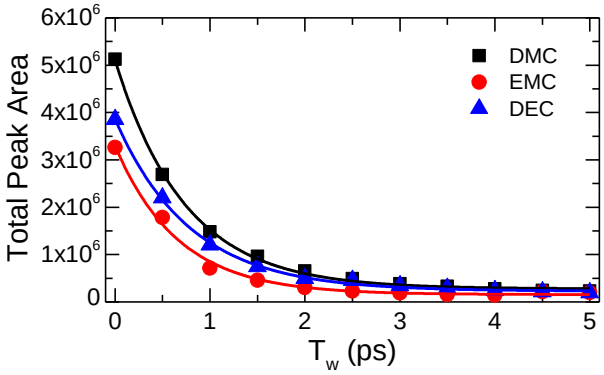

Figure S11. Vibrational lifetimes of the coordinated carbonyl stretch mode in the three electrolytes as determined by the absolute value of the total intensity of the Li^+-coordinated band in the 2DIR spectra as a function of T_w.

TABLE S5. Results of modeling the vibrational lifetimes shown in Figure S6 with exponential growth functions of the form: $\boldsymbol{A * e^{-T_w/T_1} + y0}$.

	y0	A	T_1 (ps)
DMC	2.8e5±0.2e5	4.83e6±0.05e6	0.74±0.02
EMC	1.5e5±0.3e5	3.15e6±0.08±6	0.66±0.04
DEC	2.3e5±0.2e5	3.53e6±0.04e6	0.79±0.02

Li^+-O distance potential

The potential for the Li^+-O distance (dr) was calculated from gas phase DFT calculations for DMC. The Li^+--O=C angle (θ) was restricted to the value obtained for the optimized geometry: θ = 148.1°.

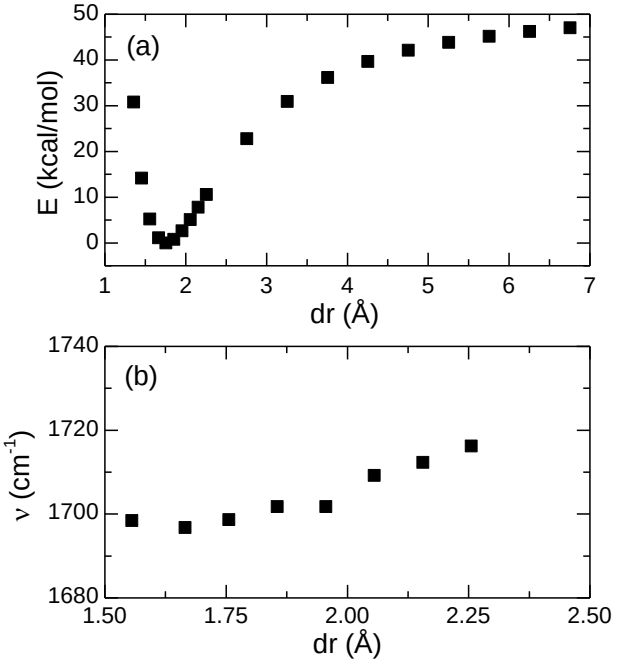

Figure S13. (a) Calculated potential for the Li^+-O distance (dr). Note that the energy scale was adjusted vertically such that the minimum energy is 0 kcal/mol. (b) Calculated frequency of the coordinated carbonyl stretch as a function of Li^+-O distance (dr).

Calculated Relative Cross Peak Intensities

Using gas phase density functional theory, the frequencies and intensity of the carbonyl stretches from the optimized Li^+ solvation shells formed by each of the three linear carbonates were computed. The relative cross peak intensities were calculated and compared with the experimentally measured relative cross peak intensities at zero waiting time using the following relationship:

$$\frac{\mu_s^2}{\mu_{a_1}^2 + \mu_{a_2}^2 + \mu_{a_3}^2} \cong \frac{I_s}{I_{a_1} + I_{a_2} + I_{a_3}}$$

There is good agreement between the experimental relative cross peak intensities and the calculated cross peak intensities, indicating that the distortions of the solvation shell caused by the alkyl chains of the various carbonates are well represented in the calculated solvation structures.

TABLE S6. Calculated and experimentally measured relative cross peak intensities for the DMC, EMC, and DEC electrolytes.

Solvent	Calculated	Experimental
DMC	0.10	0.12
EMC	0.09	0.13
DEC	0.09	0.09

Modeling of the Cross Peak Growth

In order to properly model the cross peak growth, a kinetic model which accounts for all process leading to energy transfer in a system of coupled vibrational oscillators is required.[3]

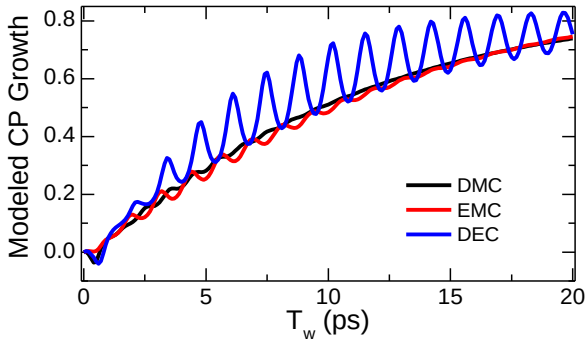

Figure S14. Model of cross peak growth in each electrolyte extended to 20 ps.

1. R. Aroca, M. Nazri, G. A. Nazri, A. J. Camargo and M. Trsic, *J. Solution Chem.*, 2000, **29**, 1047-1060.
2. L. Doucey, M. Revault, A. Lautie, A. Chausse and R. Messina, *Electrochim. Acta*, 1999, **44**, 2371-2377.
3. A. Ghosh, M. J. Tucker and R. M. Hochstrasser, *J. Phys. Chem. A*, 2011, **115**, 9731-9738.